Atmos. Chem. Phys. Discuss., doi:10.5194/acp-2015-990, 2016
Manuscript under review for journal Atmos. Chem. Phys.
Published: 5 February 2016

Atmospheric Chemistry and Physics Discussions

New particle formation in the fresh flue gas plume increase the effective particle number emissions of a coal-fired power plant

Fanni Mylläri[1], Eija Asmi[2], Tatu Anttila[1], Erkka Saukko[1], Ville Vakkari[2], Liisa Pirjola[3], Risto Hillamo[2], Tuomas Laurila[2], Anna Häyrinen[4], Jani Rautiainen[4], Heikki Lihavainen[2], Ewan O'Connor[2], Ville Niemelä[5], Jorma Keskinen[1], Miikka Dal Maso[1], and Topi Rönkkö[1]

[1]Department of Physics, Tampere University of Technology, P.O. Box 692, FI-33101 Tampere, Finland.
[2]Atmospheric Composition Research, Finnish Meteorological Institute, FI-00560, Helsinki, Finland.
[3]Department of Technology, Metropolia University of Applied Sciences, FI-00180, Helsinki, Finland.
[4]Helen Oy, FI-00090 Helen, Helsinki, Finland
[5]Dekati Ltd., Tykkitie 1, 36240 Kangasala, Finland

Correspondence to: Topi Rönkkö (topi.ronkko@tut.fi)

Abstract. Atmospheric emissions, including particle number and size distribution, of a 726 MW_{th} coal-fired power plant were studied experimentally from power plant stack and from flue gas plume dispersing in the atmosphere. Experiments were conducted under two different flue gas cleaning conditions. The results were utilised in a plume dispersion and dilution modelling taking into account nucleation particle precursor (H_2SO_4 resulted from the oxidation of emitted SO_2) formation and assessment related to nucleation rates. The experiments showed that the primary emissions of particles and SO_2 were effectively reduced by flue gas desulphurization and fabric filters, especially the emissions of particles smaller than 200 nm in diameter. Primary pollutant concentrations reached background levels in 200–300 seconds. However, the atmospheric measurements indicated that new particles are formed in the flue gas plume, even in the very early phases of atmospheric ageing. The effective number emission of nucleated particles were several orders of magnitude higher than the primary particle emission. Modelling studies indicate that regardless of continuing dilution of the flue gas, nucleation precursor (H_2SO_4 from SO_2 oxidation) concentrations remain relatively constant. In addition, flue gas nucleation is more efficient than natural atmospheric nucleation. Especially, the observation of the new particle formation with rather low flue gas SO_2 concentrations changes the current understanding on the air quality effects of coal-combustion. The results can be used to evaluate the optimal ways to achieve better air quality particularly in polluted areas like India and China.

Atmos. Chem. Phys. Discuss., doi:10.5194/acp-2015-990, 2016
Manuscript under review for journal Atmos. Chem. Phys.
Published: 5 February 2016

Atmospheric Chemistry and Physics Discussions

1 Introduction

In global scale, nearly 40 % of annual production of electricity is covered by coal combustion (EU, 2014). In addition to CO_2 emissions, known to have climatic effects, coal combustion causes emissions of other harmful pollutants like NO_x, SO_2, and particles, all decreasing the air quality and increasing health related risks but also affecting climate. Coal combustion related air quality problems exist especially in developing countries like China (Huang et al., 2014) where the power production is not always equipped with efficient flue gas cleaning systems. However, with proper combustion and flue gas cleaning technologies the fine particle emissions of coal combustion can be decreased to very low level and also the emissions of gaseous pollutants other than CO_2 can be decreased. Particle mass and number emission factors for the 300 MW coal-fired power plant with electrostatic precipitator (ESP) and flue gas desulphurization unit (FGD) have been reported by Frey et al. (2014): the emission for particle mass (PM1) was 0.18 ± 0.06 mg MJ^{-1} and for fine particle number $2.3{\cdot}10^9$ $\pm$ $4.0{\cdot}10^9$ MJ^{-1}. However, it can be expected that particle emissions and also the characteristics, such as particle size, are highly dependent on technologies used in the power production. Only few studies have reported particle number size distributions and mean particle diameter for the coal combustion emissions. The mean particle diameters have been reported to be between 100 nm (Frey et al., 2014; Yi et al., 2008) and 1 μm (Yi et al., 2008; Lee et al., 2013). According to Saarnio et al. (2014), chemical composition of particles in the efficiently cleaned flue gas after the FGD is shifted towards desulphurization chemicals. Interestingly, sulphate particle emissions from coal combustion with proper cleaning technologies can restrain the global warming due to cooling effect of the particles (Frey et al., 2014; Charlson et al., 1992; Lelieveld et al., 1992).

Due to the emission limits of power plants, driven by needs for healthier environment, emissions should be kept at minimum. This can be achieved by different technologies. Flue gas NO_x emissions can be reduced in the power plant boiler by applying low-NO_x burners, whereas SO_2 emissions can be reduced by flue gas desulphurization (FGD) (Srivastava et al., 2001). Particle emissions can be reduced by electrostatic precipitators (ESP) and fabric filters (FF). Very low emission levels can be achieved by these techniques. For example from particle emission point of view, ESP typically removes 99% (Helble, 2000) of the fine particles. Further, Saarnio et al. (2014) showed that desulphurization plant with fabric filters remove up to 97 % of the fine particles. Combination of these techniques would then remove 99.97 % of the fine particle emissions of the particles formed in combustion. However, particle emission as well as the effects of technologies can differ from these if the emissions are measured from the diluted flue gas in the atmosphere. In principle, particle number and even particle mass can increase in the atmosphere for example due to the nucleation and condensation processes (Marris et al., 2012; Buonanno et al., 2012). However, there are very few observations of the processes in the diluting flue gas during the first few minutes after the stack.

Power plant plumes have been studied with aircrafts by measuring long distance cross-wind profiles of gases and particles (Stevens et al., 2012; Brock et al., 2002; Lonsdale et al., 2012; Junkermann

Atmos. Chem. Phys. Discuss., doi:10.5194/acp-2015-990, 2016
Manuscript under review for journal Atmos. Chem. Phys.
Published: 5 February 2016

Atmospheric Chemistry and Physics Discussions

et al., 2011). Stevens et al. (2012) and Lonsdale et al. (2012) have compared these measurements to modelling results, which were based on emission inventory values. Modelling results indicated that secondary particle formation occurs in the plumes after 10–20 km from the stack, whereas Brock et al. (2002) argue the secondary particle formation to begin at 2 hour aged plume. Study of Brock et al. (2002) has focused on plume ages 0 to 13 hours old power plant plumes. However, Brock et al. (2002) do not report particle number concentrations for fresh flue gas. Cross-wind profiles shown in the study of Stevens et al. (2012) were from 5 km to a bit over 50 km distances, and these results were also used in Lonsdale et al. (2012). On the contrary, Junkermann et al. (2011) followed the plume centre line based on the SO_2 concentrations and made also few cross-wind profiles of the studied plume.

This study focuses on real atmospheric dilution and dispersion of CO_2, SO_2 and particles emitted from a 726 MW coal-fired power plant. The power plant has two boilers with separate flue gas cleaning systems. The measurement equipment was installed into two locations; into a helicopter, which enabled the measurement of real flue gas plume in the atmosphere, for the first time, and into the stack. The measurements in the flue gas plume and in the stack were conducted for two different flue gas cleaning situations, i.e. when the flue gas desulphurization unit including fabric filters was in operation (later called as "FGD+FF on") and when it was bypassed (later called as "FGD+FF off"). The measurement of flue gas plume enabled studying the aerosol processes and flue gas dilution as a function of time and also in the vicinity of the source (from tens of meters to kilometers). The study comprises measurements made in the stack and in the flue gas plume with dispersion and aerosol process modelling.

2 Experimental

The studied power plant is a base-load station located near Helsinki city centre, Finland. The power plant consists of two 363 MW_{th} coal-fired boilers. The energy is produced by coal combustion in 12 low-NO_x technology burners (Tampella/Babcock-Hitachi HTNR low NO_x), situating at the front wall of the boiler. The properties of coal used in this study are listed in SI1. Combustion releases flue gases that are cleaned in electrostatic precipitator (ESP), semi-dry desulphurization plant (FGD), and fabric filters (FF) before the stack. There are separate flue gas ducts and flue gas cleaning systems for each boiler.

The flue gas was studied in two different locations: the flue gas plume, and a reference point inside the stack. Measurements were made at both locations with two different flue gas cleaning situations: "FGD+FF off" and with all cleaning systems ("FGD+FF on"). The measurement location in the stack was at the height of +35 meters above sea level. The flue gas temperature inside the duct was 78 $\pm$ 2 °C in normal operation conditions and 130 $\pm$ 13 °C during "FGD+FF off" situation. The flue gas plume concentrations were measured with a helicopter equipped with aerosol instruments.

Atmos. Chem. Phys. Discuss., doi:10.5194/acp-2015-990, 2016
Manuscript under review for journal Atmos. Chem. Phys.
Published: 5 February 2016

Atmospheric Chemistry and Physics Discussions

The flying altitude of the helicopter was 150 meters above ground level or higher which corresponds to the LIDAR (Halo Photonics Streamline Doppler lidar with full-hemispheric scanning capability) (SI2) results for plume altitude. It should be noted that only the flue gases from the boiler under investigation were steered to bypass FGD and FF. Thus, in the "FGD+FF off" situation flue gas plume consisted of both the cleaned flue gas and the flue gas cleaned by ESP. This has to be kept in mind in the analysis of atmospheric measurements.

Weather conditions were quite stable during the study. The wind direction and speed were 210 ° and 6.5 m s^{-1} in "FGD+FF off" case and 260 ° and 4 m s^{-1} in "FGD+FF on" case, respectively. The marine boundary layer height was 246–258 meters and the planetary boundary layer heights were 360–530 meters. However the calculations were made within the marine boundary layer because the flue gas plume did not arise above it. The background aerosol concentrations for each measured gaseous component were: CO_2 403 ppm, SO_2 less than 2–8 ppb. The ambient temperature was 6.6–6.9 °C, the global radiation was 346–466 W m^{-2} and the visibility was over 30 000 meters.

The instrument installations in different locations are shown in SI3. The sampling of flue gas in the stack was performed with Fine Particle Sampler (FPS; Dekati Ltd.) with total dilution ratio (DR) of 27. Probe and dilution air temperatures were at 200°C. The sample was led to instruments: Condensation Particle Counter (CPC3776; TSI Inc.), ELPI (Dekati Ltd.), SMPS 0.6/6 slpm (DMA3071, CPC3775 TS Inc.) and gas analysers for diluted CO_2 (model VA 3100, Horiba) and NO, NO_2 and NO_x (model APNA 360, Horiba). Measurement data was also received from a normal operation monitoring of the emissions, including raw flue gas SO_2, NO_x, CO_2 concentrations and dust (SICK RM 230, calibrated based on SFS-EN 13284-1 standard). In contrast to stack sampling, the sample in the flue gas plume dilutes naturally and can be sampled to equipment without additional dilution of aerosol sample. The sampling inlet position in the helicopter is shown in S3. Natural dilution causes rapid changes in concentrations and, thus, high measurement frequency equipment were used in the helicopter. CPC3776 (TSI Inc.) was installed to measure the total particle number concentration, whereas Engine Exhaust Particle Sizer (EEPS, TSI Inc.) was measuring the particle number size distribution at 1 Hz sampling frequency. Gas concentrations for CO_2/CH_4/H_2O (Cavity spring-down spectrometry Picarro model G1301-m CO_2/CH_4/H_2O Flight Analyzer) and SO_2 (Thermo Scientific Inc. model 43i SO_2 analyzer, with 5 second response time) were measured continuously with 1 Hz frequency.

Fig. 1 shows the helicopter measurement routes for "FGD+FF on" and "FGD+FF off" situations. The objective of flight routes was to follow the centre line of the flue gas plume. Helicopter flew both up and down of the plume; the gps-data was used to separate these two flight situations to calculate the distance and the age of the plume separately.

Atmos. Chem. Phys. Discuss., doi:10.5194/acp-2015-990, 2016
Manuscript under review for journal Atmos. Chem. Phys.
Published: 5 February 2016

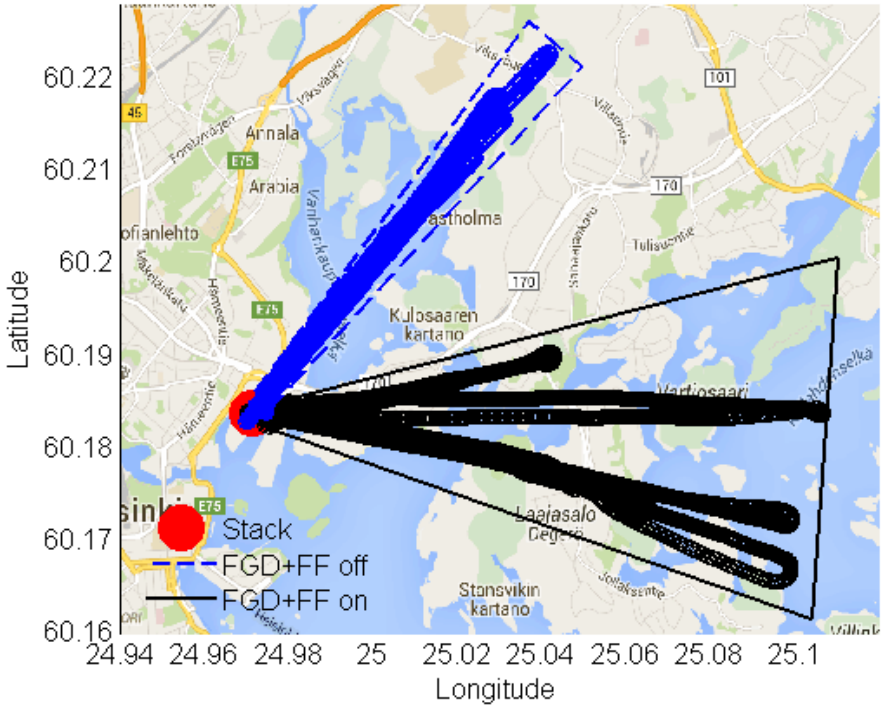

Figure 1. Helicopter flight routes. The wind blew 210° angle in "FGD+FF off" and 260 ° in "FGD+FF on" case.

2.1 Model description: Gaussian plume model

The Gaussian plume model is a solution to an advection-diffusion equation that describes the changes in the pollutant concentrations due to advection of wind and turbulent mixing with the surrounding air (Stockie, 2011). Accordingly, the concentration of a pollutant i, C_i, emitted from a point-like source, can be expressed as follows:

$$C_i(x,y,z) = \frac{Q_i}{2\pi U \sigma_y \sigma_z} \exp(-\frac{y^2}{\sigma_y^2})[\exp(-\frac{(z-H)^2}{\sigma_z^2}) + \exp(-\frac{(z+H)^2}{\sigma_z^2}] \quad (1)$$

Here x, y and z are the spatial coordinates, aligned so that x axis corresponds to the wind direction, and H is the height at which i is emitted (stack height). Also, Q_i is the emission rate of i at the source, U is the mean wind speed, and σ_z as well as σ_y are the so called dispersion coefficients which reflect the spatial extent of the plume as a function of the downwind distance x. The dispersion coefficients were calculated using the parameterization of Klug (1969) and the atmospheric stability class, which is needed to calculate the dispersion coefficients. Atmospheric stability classes were estimated based

Atmos. Chem. Phys. Discuss., doi:10.5194/acp-2015-990, 2016
Manuscript under review for journal Atmos. Chem. Phys.
Published: 5 February 2016

Atmospheric Chemistry and Physics Discussions

on the measurements of the wind speed and solar radiative flux at the surface. Moreover, the pollutant concentrations were calculated along the centerline of the plume, the value of U was set to constant and equal to the average wind speed during the flights. Finally the value of z was set equal to the stack height (150 meters).

It is worth noting that the background concentration of i is zero according to eq. 1: $C_i \rightarrow 0$ when $z \rightarrow \infty$ or $y \rightarrow \pm\infty$ However, the flue gas emitted from the stack was actually cleaner, in terms of particle number concentration, than the background air when the flue gas was cleaned properly. In order to take into account for such cases, the following equation was used instead of eq. 1:

$$\hat{C} = C_\infty + \frac{C_0 - C_\infty}{C_0} \cdot C_i \quad (2)$$

where C_∞ is the background concentration of i, and C_0 is its concentration at the source. It can be readily shown that eq. 2 is a solution the advection-diffusion equation underlying eq. 1. Also, it is easily verified that $\hat{C} \rightarrow C_\infty$ when $z \rightarrow \infty$ or $y \rightarrow \pm\infty$. Finally, the value of Q_i in eq. 1 was chosen so that $\hat{C} \rightarrow C_0$ when $z \rightarrow H$ and x,$y \rightarrow 0$.

An important output of the model is the dilution ratio of the flue gas plume, DR, which is calculated as follows DR(t)= ([$CO_2(t)$] - [$CO_{2,\infty}$])/([$CO_{2,stack}$]- [$CO_{2,\infty}$]) where [$CO_2(t)$] and [$CO_{2,\infty}$] are the modelled CO_2 concentration at time t and the CO_2 concentration measured in the stack, respectively.

2.1.1 Model description: Nucleation rate and particle formation calculations

The particle appearance (driven by nucleation and growth) rates at the lowest diameter detected by the CPC (2.5 nm) were calculated using the parameterization developed by Lehtinen et al. (2007). The key input parameters for the model are the nucleation rate (J_{nuc}), the particle growth rate (GR), and the coagulation sink which describes the rate at which clusters are removed via coagulational scavenging ($CoagS$). The parameter J_{nuc} is calculated based on the estimated sulphuric acid concentrations as function of plume age as detailed below, and the particle growth rates are calculated by assuming growth only via irreversible condensation of sulphuric acid. Also, $CoagS$ is calculated from the condensation sink CS (which is calculated in a fashion described below) using the eq. 8 in Lehtinen et al. (2007). Also, the initial size of the freshly nucleated clusters was varied, and the value of the shape factor (m in Eq. 6 in Lehtinen et al. (2007)) was set equal to –1.6.

The nucleation rates J_{nuc} in the studied plume were calculated using the parameterization developed by Kulmala et al. (2006) which has also been applied previously to model nucleation in plumes (Stevens et al., 2012, 2013). Accordingly, J_{nuc} = A×[H_2SO_4] where A=1·10^{-7} s^{-1} or A=1·10^{-6} s^{-1} and [H_2SO_4] (cm^{-3}) is the sulphuric acid concentration. The value of A=1·10^{-7} s^{-1} was chosen according to the study of Stevens et al. (2012, 2013).

Formation of [H_2SO_4] was calculated assuming that it is produced only via the OH + SO_2 reaction and the only loss pathway for H_2SO_4 is condensation onto the particle surfaces. When steady-state

Atmos. Chem. Phys. Discuss., doi:10.5194/acp-2015-990, 2016
Manuscript under review for journal Atmos. Chem. Phys.
Published: 5 February 2016

Atmospheric Chemistry and Physics Discussions

is assumed, the following equation is thus obtained $[H_2SO_4] = k_1 \times [SO_2] \times [OH]/CS$ where k_1 is the reaction constant between OH and SO_2 (Table B.2 in Seinfeld and Pandis, 2008). The SO_2 concentrations were taken from the helicopter measurements, and the time development of CS and [OH] in the plume were modelled as follows. First, CS was calculated using the relation $CS = CS_{stack}/DR + CS_\infty \times (1 - 1/DR)$ where CS_{stack} is the condensation sink of aerosols measured in the stack, and CS_∞ is the condensation sink of the background aerosols. The value of the latter parameter was calculated from the size distributions measured at the SMEAR III station (Junninen et al., 2009) which is located around two kilometers away from the power plant. Second, [OH] was calculated using the parameterization of Stevens et al. (2012) which has downward shortwave radiative flux at the surface and $[NO_x]$ as main inputs. Value for the former parameter was taken from the measurements (using the value averaged over the measurement periods), and the NO_x concentrations were calculated as follows: $[NO_x(t)] = [NO_{x,stack}]/DR(t)$ where $[NO_{x,stack}]$ is the NO_x concentration measured in the stack. It should be noted here that in the calculations the background concentration of NO_x is assumed to be of minor importance when compared to NO_x emitted by power plant. To support this, the study of Pirjola et al. (2014) indicates that in the harbour area close to the power plant studied here the NO_x concentration level is typically clearly lower than 100 ppb.

3 Results

3.1 Primary emissions of the coal-fired power plant

The SO_2 and particle emissions of the power plant were strongly dependent on flue gas cleaning system. This can be seen in Table 1 which shows flue gas concentrations for CO_2, SO_2, NO_x, O_2, particle number (N_{tot}), dust as well as flow rate in the duct in both flue gas cleaning conditions. In the shift from "FGD+FF off" to "FGD+FF on" situation the SO_2 concentration decreased nearly to fifth part, the concentration of dust decreased by a factor of 50 and the N_{tot} decreased by a factor of four thousand. For other parameters the effect of FGD+FF was insignificant.

Figure 2 shows the particle number size distributions of flue gas in the stack in both cleaning conditions. These were measured using an electrical low pressure impactor (ELPI) and a scanning mobility particle sizer (SMPS) in both "FGD+FF on/off" cases. In the "FGD+FF on" case the SMPS measurement is a median value over few hours of operation due to low particle number concentrations in the stack. Based on the SMPS measurement the particle mean mobility diameter was 80 nm and the width of particle number size distribution (geometric standard deviation, GSD) was 1.45 for "FGD+FF off" case. In comparison, the mean mobility diameter was 31 nm for "FGD+FF on" and the width of particle number size distribution was 2.15. Based on the measurements using the ELPI mean aerodynamic diameter was 141 nm and GSD was 1.41. The difference in mean diameters measured using the ELPI and the SMPS comes from the size classification principle of the ELPI, which is sensitive to particle density. In fact, the difference indicates effective density larger than unit

Atmos. Chem. Phys. Discuss., doi:10.5194/acp-2015-990, 2016
Manuscript under review for journal Atmos. Chem. Phys.
Published: 5 February 2016

Atmospheric Chemistry and Physics Discussions

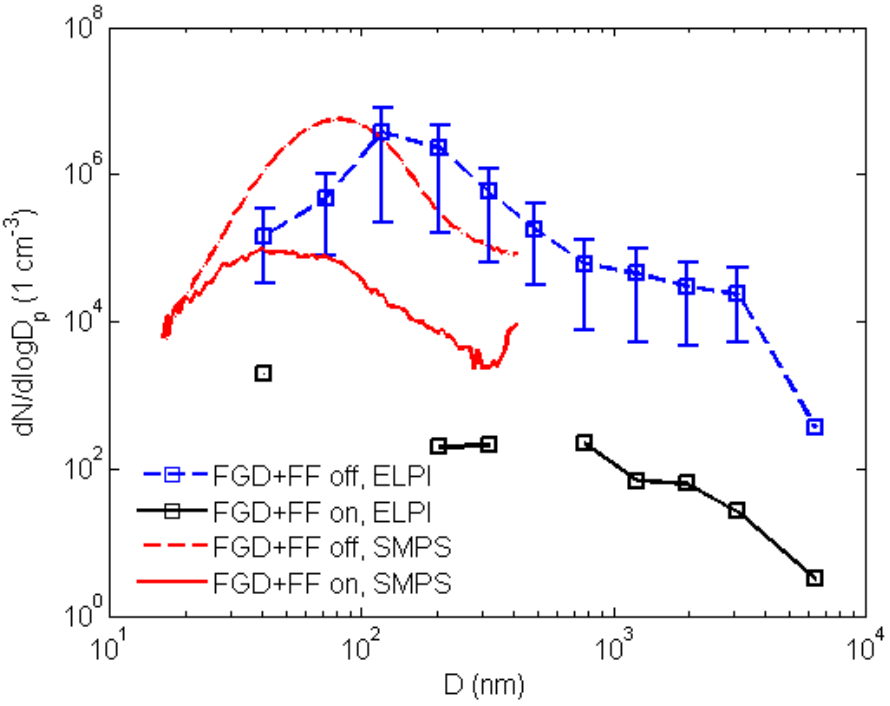

Figure 2. Particle size distributions measured with ELPI and SMPS from the flue gas in the stack. ELPI and SMPS data is shown in operation conditions, "FGD+FF on" and "FGD+FF off". The x-axis is aerodynamic diameter for ELPI data and electrical mobility diameter for SMPS data.

density for emitted particles (approximately 3.1 g cm^{-3}). In comparison, Saarnio et al. (2014) used effective density of 2.5 g cm^{-3} to convert the electrical mobility diameter measured using SMPS to aerodynamic diameter. When studying "FGD+FF on" case there was no difference between aerodynamic particle diameter and mean mobility diameter and, thus no difference in the density of the particles.

Flue gas sample from the stack was diluted with hot dilution air before the particle instruments and thus the particle number concentrations (Table 1) and particle size distributions (Figure 2) are for non-volatile particles. In combustion studies the hot dilution air is typically used to prevent the formation of liquid nucleation particles and to minimize the effects of condensation of semi-volatile compounds on particles. However, to ensure the measured particles were non-volatile and not affected by the dilution method itself, a thermodenuder (Rönkkö et al., 2011) was used periodically after the sampling and dilution. The thermodenuder did not affect the particle number size distribution, which confirms the non-volatile nature of the measured particles. Due to this non-volatility of

Atmos. Chem. Phys. Discuss., doi:10.5194/acp-2015-990, 2016
Manuscript under review for journal Atmos. Chem. Phys.
Published: 5 February 2016

Atmospheric Chemistry and Physics Discussions

Table 1. Flue gas concentrations of CO_2, SO_2, NO_x, O_2, total particle number (N_{tot}), dust, and flue gas flow rate in the stack. Mean values (+ standard deviation) are presented for both flue gas cleaning conditions ("FGD+FF on" and "FGD+FF off").

	FGD+FF off	FGD+FF on
CO_2 (%)	9.92 ± 2.2	10.3±0.96
SO_2 (ppm)	243±71.3	55.2±1.46
NO_x (ppm)	252±74	258±65
O_2 (%)	6.16±0.11	6.11±0.10
N_{tot} (cm^{-3})	$(1.8 \pm 0.2) \cdot 10^6$	420±640
Dust (mg/Nm^3)	188±82	4±1
Flow (Nm^3/h)	$(4.86 \pm 0.20) \cdot 10^5$	$(4.65 \pm 0.064) \cdot 10^5$

the particles, the life time of the primarily emitted particles in the atmosphere can be longer than that of volatile particles, e.g. nucleation mode particles observed in vehicle exhaust (Lähde et al., 2009).

3.2 Atmospheric measurements

The measurement results are shown in Figure 3 describing the flue gas plume concentrations as a function of plume age. The data was recorded based on gps-coordinates which were used to calculate distances from the stack, and the distances were changed to correspond plume age using wind speeds 6.5 m s^{-1} and 4.0 m s^{-1} (LIDAR, S3). The vertical lines denote the 2 km distance from the stack. Figure 3 shows the dilution time scale of the flue gas in terms of CO_2 and SO_2 in both operation conditions. Same trend in SO_2 and N_{tot} concentrations as observed in Table 1, was measured by instruments installed in the helicopter; in "FGD+FF off" situation the particle and SO_2 concentrations were higher than the "FGD+FF on" situation. It should be kept in mind that in "FGD+FF off" situation only one of the two flue gas cleaning systems was bypassed.

Plume dilution can be evaluated by the CO_2 concentrations (in Figure 3 a and b), which show that the "FGD+FF off" case dilutes to approximately background level in 200 seconds (0.74 km) and the "FGD+FF on" case in 300 seconds (1.5 km). The peak values for CO_2, SO_2 and N_{tot} were 3195 ppm, 2193 ppb, $3.\cdot 10^4$ cm^{-3} in the "FGD+FF off" situation and 3254 ppm, 585 ppb, $0.4\cdot 10^4$ cm^{-3}, respectively, for the "FGD+FF on". However, the dilution decreases the CO_2, SO_2 and N_{tot} concentrations in the atmosphere to 422 ppm, 52 ppb in "FGD+FF off" situation, and 473 ppm, 89 ppb in"FGD+FF on" situation. Respectively, the N_{tot} reached nearly to background concentrations after 200 seconds and 300 seconds. The background concentrations for each measured gaseous component were 403 ppm and < 25 ppb, for CO_2 and SO_2 respectively. The boundary layer mixing started during the "FGD+FF on" measurements and thus the closest background values were subtracted from both "FGD+FF on/off cases". It can be noted that very near (first 10–50 seconds) the stack the helicopter was not in the plume. This can be seen from CO_2 and SO_2 concentration values presented

Atmos. Chem. Phys. Discuss., doi:10.5194/acp-2015-990, 2016
Manuscript under review for journal Atmos. Chem. Phys.
Published: 5 February 2016

Atmospheric Chemistry and Physics Discussions

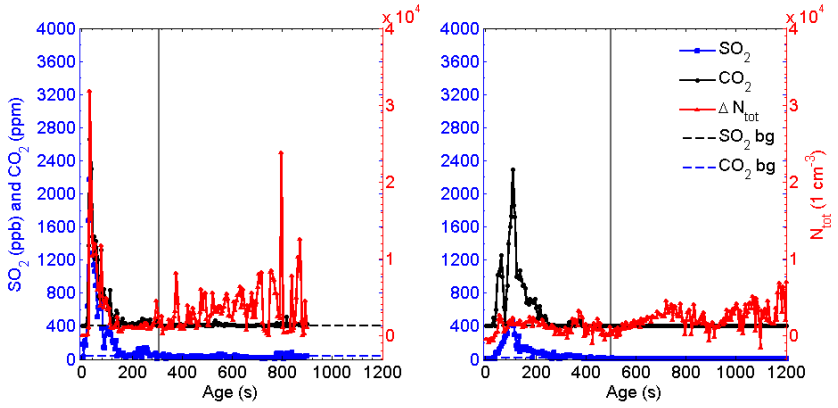

Figure 3. Concentrations of power plant flue gas components measured by instrument installed in to the helicopter as a function of plume age; "FGD+FF off" on the left and "FGD+FF on" on the right. SO_2 (ppb, black line) and CO_2 (ppm, blue line) concentrations on the left axes and total particle number concentration ΔN_{tot} (1 cm^{-3}, red line) on the right axes. The ΔN_{tot} is calculated using the closest background value. The grey vertical lines denote 2 km distance from the stack in "FGD+FF on/off" cases. The presented results are 5 second median values.

in Figure 3a and 3b when approaching plume age zero. Thus, the dilution process is discussed below, mainly, from the maximum concentrations forward.

An increase in total particle concentration can be seen in Figure 3 after 400 seconds aged the flue gas plume. This tendency can be seen in both flue gas cleaning situations. Based on Figure 3a, for "FGD+FF off" case the background particle concentration was 1430 cm^{-3}, after 200 seconds the concentration was at the background level and after 400 seconds it increased to 10 000 cm^{-3}. Based on CO_2 measurements, the dilution of flue gas was practically complete at 200 seconds. Similarly, in "FGD+FF on" case after 500 seconds the particle concentration was slightly above background, after which increasing even up to 5 000 cm^{-3} after 700 seconds. Thus, the concentrations in the diluted and aged flue gas plume were higher than the background and significantly higher than could be expected based on the primary particle concentrations and observed dilution profiles. There is a moderate increase in CO_2, and SO_2 concentrations at 350 sec in "FGD+FF on" case and at 250 seconds (SO_2, CO_2 and N_{tot}) in "FGD+FF off" case (Figure 3). The moderate increase in "FGD+FF on" case can be seen in EEPS data (Figure 4) but not in "FGD+FF off" case. To authors knowledge the moderate peaks cannot be explained by additional external emission sources because there should not be any sources at the same altitude in the flight directions (Figure 1) or upwind of the plume direction. Thus, the increased concentrations seem to be caused by occasionally different plume mixing. In general, taking into account the fact that there is no comprehensive measurement of the primary precursor matrix (only [SO_2] is measured), the primary precursor matrix might include low-

Atmos. Chem. Phys. Discuss., doi:10.5194/acp-2015-990, 2016
Manuscript under review for journal Atmos. Chem. Phys.
Published: 5 February 2016

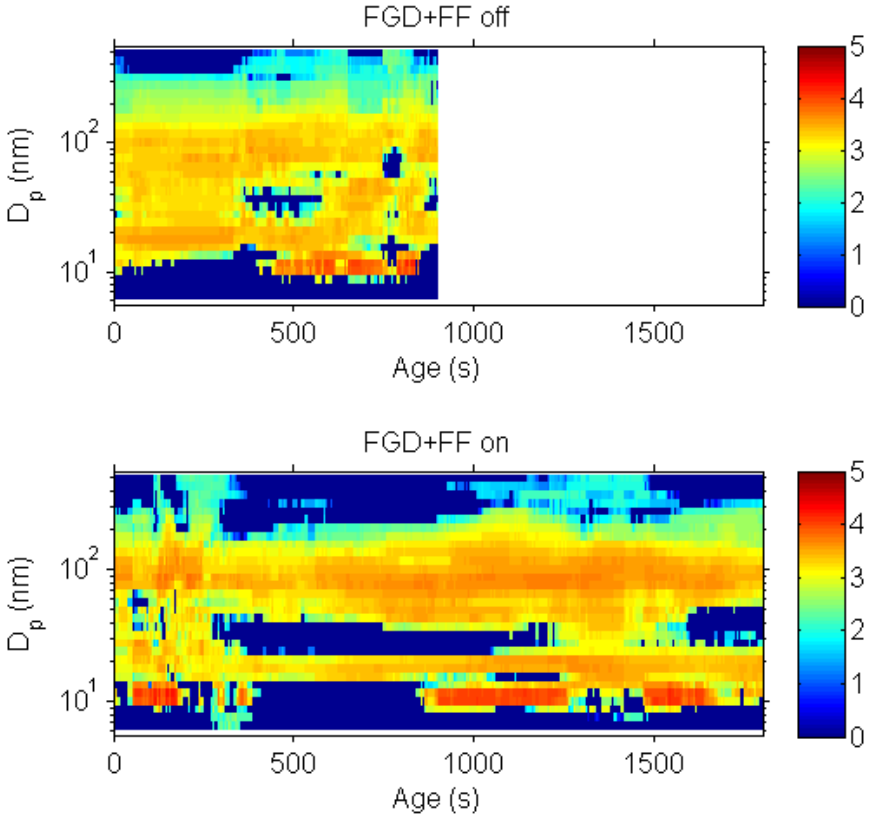

Figure 4. The particle number size distribution calculated from EEPS data as a functions of plume age. Measurement was made with the EEPS installed to helicopter. The results are calculated 10 second moving median values.

volatile organics and SO_3 which can increase the probability of new particle formation. Due to the increasing trend in particle concentration, some estimation about nucleation rates can be calculated. Depending on the plume age the mean nucleation rates calculated from the data shown in Figure 3 depended on the plume age being for "FGD+FF off" case 0–81 cm^{-3} s^{-1} and for "FGD+FF on" case 0 cm^{-3} s^{-1} to 18 cm^{-3} s^{-1} (average change in total particle number concentration at 400–482 s and 500–692 s).

Figure 4 shows the flue gas plume particle number size distribution as a function of plume age. Distributions were calculated from the EEPS data measured from the helicopter in both "FGD+FF on/off" situations as 10 second moving median method. In Figure 4 the freshly emitted plume par-

Atmos. Chem. Phys. Discuss., doi:10.5194/acp-2015-990, 2016
Manuscript under review for journal Atmos. Chem. Phys.
Published: 5 February 2016

Atmospheric Chemistry and Physics Discussions

ticle size distribution in "FGD+FF off" case is changing in same ages than N_{tot} concentrations in Figure 3. The particle size distribution had a mode around 80 nm, which refers to the solid particle median diameter measured with the SMPS from the flue gas in the stack. Figure 4 indicates similar dilution profile for particles, if N_{tot} is calculated from EEPS data, than the dilution was for CO_2 and SO_2 in Figure 3. The comparison between CPC (Figure 3) and EEPS particle size distribution (Figure 4) shows that the flue gas is diluting in 0–300 seconds in "FGD+FF off " and 0–550 seconds in "FGD+FF on " and after that more small particles (and some larger particles) are detected in both cases. Although, EEPS total particle number concentration cannot be compared to total concentration of CPC because Levin et al. (2015) showed that EEPS total particle number concentration is not comparable with a CPC. Further, the Figure 4 the EEPS particle size distribution data is noisy and based on Awasthi et al. (2013) can show maximum of 67 % wrong compared to SMPS.

3.3 Model Calculations: Modelled vs measured CO_2 concentrations

The validity of the Gaussian plume model was tested against CO_2 measurements from the plume. Median CO_2 concentrations were calculated using the measurement data at a five seconds interval separately for the "FGD+FF on/off" cases, and the locations of the peak CO_2 concentration (tmax, $[CO_{2,max}]$) were identified from the resulting time series. The value C_0 was chosen to eq. 2 so that the modelled CO_2 concentration, $\hat{C}_{CO2}$, was around $[CO_{2,max}]$ when $t = t_{max}$. The choice of C_0 was made in this manner rather than initializing the model to use the stack concentrations due to the following two reasons. First, Gaussian plume model does not yield reliable results close, i.e. within a few tens of meters, to the source (Arya, 1995). Second, the comparison of the results near (first 10–50 seconds) the source is problematic because the helicopter was not located at the plume centerline during the initial stages of the measurements.

Comparison of the measured and modelled CO_2 concentrations is shown in Figure 5. The chosen stability classes were 'b' and 'c' as well as 'c' and 'd' for the "FGD+FF on" and"FGD+FF off" cases, respectively, corresponding to the stability conditions ranging from unstable to neutral (Pasquill, 1961). As can be seen, the model reproduces the observed trends rather well, in particular for the "FGD+FF off" case, while the model tends to slightly overestimate the observed concentrations for the "FGD+FF on" case. The modelled and measured concentrations were within one standard deviation in general. Mean relative error (MRE) and correlation coefficients (R^2) were calculated between the measured and modelled values. For the "FGD+FF off" case, MREs were between 5 and 25%, depending on the stability class, and R^2 around 0.97, respectively. Corresponding values were between 29 and 40% (MRE) and around 0.86 (R^2) for the "FGD+FF on" case. In order to further investigate the performance of the model, comparison was made between measured and modelled SO_2 concentrations. The results showed that the model consistently overestimates the SO_2 concentration in the plume, typically by a factor between 3 and 5, compared to the measured values. This difference could be partly explained by the oxidation of SO_2 because it is not taken

Atmos. Chem. Phys. Discuss., doi:10.5194/acp-2015-990, 2016
Manuscript under review for journal Atmos. Chem. Phys.
Published: 5 February 2016

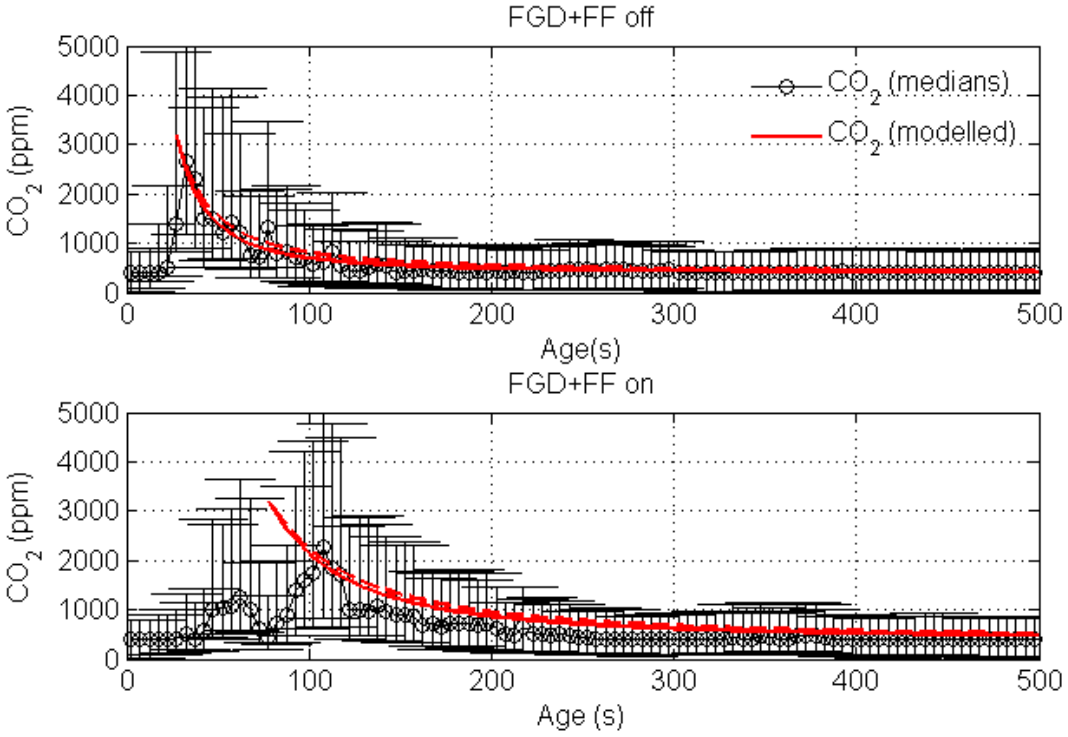

Figure 5. Comparison of measured and modelled CO_2 concentrations. Median of measured values are shown with black (circle) symbols along with the standard deviations. Dashed and dotted red lines correspond to model results for stability classes 'b' and 'c' (above) and 'c' and 'd' (below), respectively.

into account by the model. For SO_2 measurement and model comparison, the values of MRE varied between 271–578% ("FGD+FF off" case) and between 291–413% ("FGD+FF on" case), depending on the stability class. Also, R^2 was 0.93 and 0.90 for "FGD+FF off" and"FGD+FF on" cases, respectively. However, this discrepancy does not affect the model performance as the measured SO_2 concentrations, instead of modeled, were used in the plume model simulations.

3.4 Model Calculations: Nucleation and new particle formation

Modelled and measured CO_2 concentrations showed that the model reproduced the observed dispersion of the plume relatively accurately. Thus the model was applied to calculate [NO_x], [OH], and [H_2SO_4] which were needed to investigate possibility of new particle formation in the plume. These results are summarised in Figure 6. It is seen that sulphuric acid concentrations exponentially increase during the initial stages of the simulation and then reach constant concentration around $1 \cdot 10^6$

Atmos. Chem. Phys. Discuss., doi:10.5194/acp-2015-990, 2016
Manuscript under review for journal Atmos. Chem. Phys.
Published: 5 February 2016

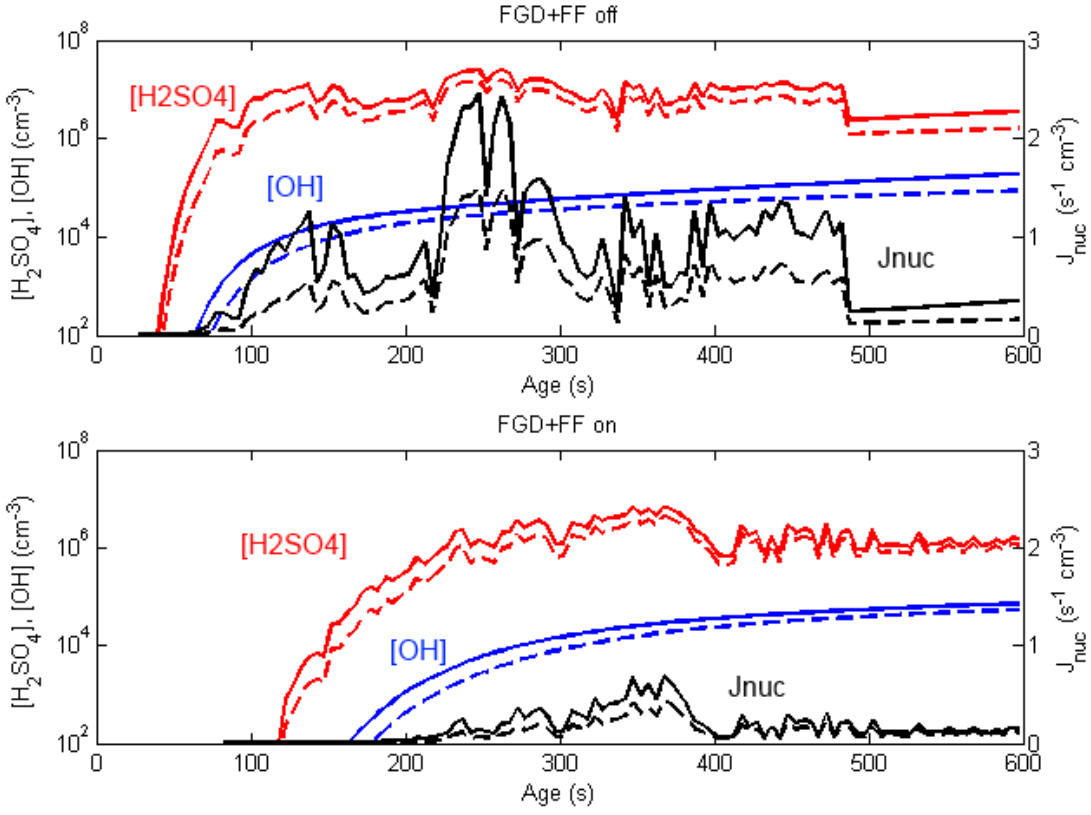

Figure 6. Time development Blue lines – [H_2SO_4], red lines – nucleation rate, black lines – [OH] (cm^{-3}). Dashed and dotted red lines correspond to model results for stability classes 'b' and 'c' (above) and 'c' and 'd' (below), respectively.

and $1{\cdot}10^7$ cm^{-3}, a range which is comparable also with the atmospheric observations of [H_2SO_4] (Mikkonen et al., 2011) formation. More H_2SO_4 is formed in the "FGD+FF off" case because of higher primary SO_2 emission compared to the "FGD+FF on" case.

Initially, OH concentrations are lowered by large concentrations of NO_x which subsequently decreases during plume ageing. NO_x reduction leads to increases in [OH] and [H_2SO_4]. While the [OH] increased consistently during the simulations, [SO_2] decreased because of dilution. Due to these opposed trends, the production term for the sulphuric acid, $k_1 \times[SO_2]\times[OH]$, did not change greatly during the later stages of the simulations. Moreover, the condensation sink (CS) diluted rapidly to its background value, which was around $1{\cdot}10^{-2}$ s^{-1}. These facts explain why the modelled

Atmos. Chem. Phys. Discuss., doi:10.5194/acp-2015-990, 2016
Manuscript under review for journal Atmos. Chem. Phys.
Published: 5 February 2016

Atmospheric Chemistry and Physics Discussions

sulphuric acid concentrations, calculated with $[H_2SO_4] = k_1 \times [SO_2] \times [OH]/CS$, did not change notably after the initial, rapid increase.

The modelled nucleation rate J_{nuc} is directly proportional to the sulphuric acid concentration and hence the trends in $[H_2SO_4]$ are directly reflected in J_{nuc} (Figure 6). The mean values of J_{nuc} were around 0.4 or 0.7 $cm^{-3}s^{-1}$, in the "FGD+FF off" case and 0.1 or 0.17 $cm^{-3}s^{-1}$ in the "FGD+FF on" case, both nucleation rates dependent on the stability class. Furthermore, apparent particle formation rate were calculated at the lowest CPC detection limit which was 2.5 nm, J25. According to the scheme applied here, fraction of freshly nucleated particles that survive into detectable sizes depends mainly on their growth rate (GR) and on the condensation sink (CS). The average GRs were 0.34 or 0.19 nm/h in the "FGD+FF off" case, and 0.07 or 0.04 nm/h in the "FGD+FF on" case; both cases are depending on the stability class. These values are clearly smaller than estimations for atmospheric observations (e.g. Kulmala et al., 2001) and thus, the modelling results do not explain the observed particle formation in the flue gas plume.

A series of additional calculations were performed in order to investigate the sensitivity of the results to the values of the key input parameters. First, J_{nuc} is proportional to the constant A whose exact value is not accurately known, and this uncertainly translates directly into the calculated nucleation rates. A sensitivity analysis was made for the nucleation model in order to evaluate the sensitivity of nucleation rates to the value of A (shown in Table 2). In these calculations, a value of $1 \cdot 10^{-6}$ was chosen for A which is an order of magnitude higher than in base case simulations. The choice of the value was based on the study of Sihto et al. (2006) who investigated NPF events occurring on boreal forest. As can be seen, increased value of A is not sufficient alone to explain observed new particle formation. A second source of uncertainty is terms of the sulfuric acid concentration which was calculated using a rather simple scheme (see section 2.1.1). Increases in $[H_2SO_4]$ leads to both increased Jnuc and GR and ultimately to larger J25. Results displayed in Table 2 show that J25 is more consistent with observations when $[H_2SO_4]$ is increased five or ten-fold and when A is set equal to $1 \cdot 10^{-6}$ like in Sihto et al. (2006). Therefore, underestimation of $[H_2SO_4]$ may explain the discrepancy between the obeservations and base case model results. This might caused by underestimation of [OH] or overestimation of CS. Regarding the modeled OH concentrations, it can be noted that they are relative low, reaching values of around $1 \cdot 10^5$ cm^{-3} by the end of the flights. In comparison, concentrations of around $1 \cdot 10^6$ cm^{-3} have been reported during the daytime around noon in various atmospheric environments (Hofzumahaus et al., 2009; Petäjä et al., 2009). Relative low modeled OH concentrations can be explained by high NO_x concentrations which were calculated to decrease consistely from several tens of ppm down to around 200 ppb during the flights (not illustrated here). Such high concentrations of NO_x are consistent with low [OH] (see Figure 1 in Lonsdale et al., 2014). It could be thus speculated that model underestimates $[H_2SO_4]$, and consequently rate of new particle formation, due to overestimation of $[NO_x]$. Moreover, it should be noted that neither SO_3 nor low-volatile organic vapours that might have been present in the measured flue

Atmos. Chem. Phys. Discuss., doi:10.5194/acp-2015-990, 2016
Manuscript under review for journal Atmos. Chem. Phys.
Published: 5 February 2016

Atmospheric Chemistry and Physics Discussions

Table 2. Sensitivity analysis made for number of particles formed with diameters above 2.5 nm during the flight ($1\ cm^{-3}$ $(600\ s)^{-1}$) in the atmosphere with different values of A and $[H_2SO_4]$. The $[H_2SO_4]$ is calculated based on the measurement results and scaled up to test faster nucleation rate for both "FGD+FF on" and "FGD+FF off" cases and stability classes (sc).

		A=1 · 10^{-7} s^{-1}					
	sc	1·$[H_2SO_4]$	1.25·$[H_2SO_4]$	1.5·$[H_2SO_4]$	2·$[H_2SO_4]$	5·$[H_2SO_4]$	10·$[H_2SO_4]$
"FGD+FF off"	b	$6.02{\cdot}10^{-2}$	$3.21{\cdot}10^{-1}$	1.04	4.97	$1.73{\cdot}10^{2}$	$1.04{\cdot}10^{3}$
	c	$3.66{\cdot}10^{-4}$	$4.70{\cdot}10^{-3}$	$2.68{\cdot}10^{-2}$	$2.59{\cdot}10^{-1}$	$2.87{\cdot}10^{1}$	$2.66{\cdot}10^{2}$
"FGD+FF on"	c	0	0	0	0	$2.56{\cdot}10^{-1}$	$1.11{\cdot}10^{1}$
	d	0	0	0	0	$5.20{\cdot}10^{-3}$	1.04
		A=1 · 10^{-6} s^{-1}					
	sc	1·$[H_2SO_4]$	1.25·$[H_2SO_4]$	1.5·$[H_2SO_4]$	2·$[H_2SO_4]$	5·$[H_2SO_4]$	10·$[H_2SO_4]$
"FGD+FF off"	b	0.6	3.21	$1.04{\cdot}10^{1}$	$4.97{\cdot}10^{1}$	$1.73{\cdot}10^{3}$	$1.04{\cdot}10^{4}$
	c	$3.66{\cdot}10^{-3}$	$46.80{\cdot}10^{-2}$	0.268	2.59	$2.87{\cdot}10^{2}$	$2.66{\cdot}10^{3}$
"FGD+FF on"	c	0	0	0	$2.3{\cdot}10^{-4}$	2.56	$1.11{\cdot}10^{2}$
	d	0	0	0	0	0.052	1.04

gas were not accounted for in the modeling study. Previous studies suggest that these exhaust compounds may increase also the formation rate of nucleation particles (Pirjola et al., 2015) which may also explain the discrepancy between measurements and model calculations.

3.5 Discussion

Each power plant (over 50 MW) in EU has emission limits for SO_2, NO_2, and particle mass concentrations, for this studied power plant the limits are 600 mg Nm^{-3} (210 ppm), 600 mg Nm^{-3} (290 ppm), and 50 mg $m^{-3}n$, respectively. Comparison between Table 1 results with the emission limits above shows that the emissions were clearly below these limits when the power plant operation was normal e.g. "FGD+FF on". It was observed that these low emissions can be achieved by properly working flue gas cleaning systems. In addition to primary emissions, flue gas cleaning systems seemingly affect also the amount of $[H_2SO_4]$ of new aerosol particles, such as SO_2 which tends to oxidate in the atmosphere to SO_3 and, further, to form H_2SO_4. This study shows clearly the importance of flue gas cleaning technologies, and underlines the proper usage of the technologies when the atmospheric pollution is discussed in terms of coal combustion. E.g. according to Huang et al. (2014) in Xi'an and Beijing 37% of sulphate in the atmospheric particles is emitted from coal burning.

The power plant plume dilutes to background levels in 200 seconds which is faster than indicated in other in-flight measurements (Stevens et al., 2012; Junkermann et al., 2011). According to modelling results of Stevens et al. (2012), atmospheric new particle formation via coal combustion orig-

Atmos. Chem. Phys. Discuss., doi:10.5194/acp-2015-990, 2016
Manuscript under review for journal Atmos. Chem. Phys.
Published: 5 February 2016

inated sulphuric acid nucleation begins at 5 km distance from the source whereas the sulphuric acid formation begins right after emission. Experiments of this study indicates that the nucleation may take place in the aged plume and being the most effective after 400 seconds, corresponding approximately 2 km distance from the emission source in atmosphere. Also this distance is significantly less than 5 km distance indicated by Stevens et al. (2012). Thus, this study indicates that atmospheric nucleation in power plant plumes takes place faster than the models and measurements have suggested before. Also, it has been known that new particles form in sulphur-rich plumes (Junkermann et al., 2011), but this study shows that nucleation can take place in lower SO_2 concentrations. In general, the particle number concentrations in the urban atmosphere may be underestimated due to particle formation in power plant plumes.

In the light of the new results authors would like to distinguish the primary particle emission from the newly formed particle emission because those particles have different effects on the atmosphere and different formation mechanisms. Comparing primary particle emission with newly formed particle emission, the effects of different particles in the atmosphere could be taken into account more precisely in aerosol models or air quality assessment. For instance, in the plume for "FGD+FF off" case rough estimates can be calculated for the particle number emission (from CPC, Figure 3) per grams of CO_2 for particles existing in the plume ages of 25–55 seconds was $2.0{\cdot}10^{10}$ (g CO_2)$^{-1}$ and in ages over 400 seconds $8{\cdot}10^{10}$ (g CO_2)$^{-1}$ and, in the "FGD+FF on" case between 55–85 seconds $4{\cdot}10^{9}$ (g CO_2)$^{-1}$ and after 500 seconds $3.74{\cdot}10^{10}$ (g CO_2)$^{-1}$. In comparison, the primary emissions were $1.75{\cdot}10^{10}$ (g CO_2)$^{-1}$ for "FGD+FF off" case and $8.0{\cdot}10^{6}$ (g CO_2)$^{-1}$ for "FGD+FF on" case. Thus, new particle formation can increase the real atmospheric particle number emissions even several orders of magnitude. It should be noted that the particle formation depends strongly on the plume age, [SO_2] and primary particle concentrations, and it is possible that there are some low-volatile organics or SO_3 present at the plume affecting the nucleation.

Coal combustion is harmful for climate due to the CO_2 emission. However, also atmospheric particles affect the climate having either cooling or warming effect depending on their chemical and physical characteristics. It is known, that soot or black carbon containing particles have a warming effect on climate. This study indicated that most of the particles originated from coal combustion are formed in the atmosphere. Based on that knowledge, it can be assumed that the formed particles are more scattering than absorbing. Also, Frey et al. (2014) have shown that primary emission of the coal-fired power plant has a scattering effect, at least when compared to other combustion originated primary particles. This study gives new insights when the effects of coal combustion are studied in a global scale. Finally, the results help to understand the formation of atmospheric particles in polluted areas, such as India and China.

Atmos. Chem. Phys. Discuss., doi:10.5194/acp-2015-990, 2016
Manuscript under review for journal Atmos. Chem. Phys.
Published: 5 February 2016

Atmospheric Chemistry and Physics Discussions

4 Conclusions

Emissions of a coal-fired power plant into the atmosphere were studied comprehensively, for the first time, by combining direct atmospheric measurements, measurements conducted in the power plant stack, and modelling studies for atmospheric processes of flue gas plume. The stack measurements were made to estimate the effectiveness of flue gas cleaning technologies, such as filtering and desulphurization. It was shown that the flue gas cleaning technologies had a great effect on the SO_2 and total particle number concentrations in the primary emission. SO_2 concentration was reduced to fifth of "FGD+FF off" situation compared to "FGD+FF on" situation and the total non-volatile particle number concentration was reduced by orders of magnitude. Similar trend in primary emission reduction was detected in the atmospheric measurements. In addition, the reduction in primary emissions affects directly the concentrations of gaseous precursors (SO_2) for secondary particle formation in the atmosphere.

It was observed that the flue gas dilutes to background concentrations in 200–300 seconds. This dilution time scale is faster than reported in previous studies. However, the concentration profiles also showed an increase in particle number concentration in an aged flue gas, dilution and dispersion processes.

To validate the dilution time scale, a Gaussian model was used to calculate the dilution in the atmosphere taking into account the primary emission and weather conditions. The Gaussian model confirms the dilution time scale, and the dilution ratio could be used to calculate the theoretical maximum values for different components in the flue gas plume. Weather conditions and theoretical maximum value for [NO_x] was used to calculate the [OH] formation rate and further [H_2SO_4] formation rate. These were calculated because the measurement results showed an increase in particle number concentrations in the flue gas plume during the dilution process. The modelling results for [H_2SO_4] formation rate support the hypothesis of sulphuric acid formation, but the sulphuric acid formation itself does not totally explain the increase in the total particle number concentration, therefore, e.g. low-volatile organics may excist on the flue gas plume. The sensitivity analysis of the [H_2SO_4] formation showed that the atmospheric parametrization is not enough to explain the processes in the flue gas plume.

Comparison between the primary particles and newly formed particles, calculated based on the atmospheric results, show in the flue gas plume of coal-fired power plant the concentration of newly formed atmospheric particles can be several orders of magnitude higher than the primary particles from the flue gas duct. This is the reason why the newly formed particles should be taken into account when discussing power plant emissions in the future. The formation of these particles in the power plant plumes should be properly parametrized to implement power plants more efficiently e.g. in air quality and climate models.

It is widely known that CO_2 emissions are harmful for the climate. However, the CO_2 emission is not the only one to have effects on the climate. Other anthropogenic gases can increase the climatic

Atmos. Chem. Phys. Discuss., doi:10.5194/acp-2015-990, 2016
Manuscript under review for journal Atmos. Chem. Phys.
Published: 5 February 2016

effects. Particles contribute the climate negatively and positively depending on the particle properties in the atmosphere. This study linked with the knowledge for other atmospheric studied indicates that the atmospheric particle formed in flue gas plumes are scattering more light than absorbing and, thus adding the cooling effect of the primary emissions of a coal-fired power plant. In addition, this study brings new insight to the atmospheric effects of coal combustion, as well as helps to understand formation of atmospheric particles in polluted areas.

Acknowledgements. The study was conducted in the MMEA WP 4.5.2. of Cleen Ltd., funded by Tekes (the Finnish Funding Agency for Technology and Innovation). Authors like to acknowledge B.Sc. Anna Kuusala and Mr Joni Heikkilä for programming Matlab, Mr Aleksi Malinen for measurement help. F.M. acknowledges TUT Graduate School, KAUTE-foundation, TES-foundation for financial support. E.A. and E.O. acknowledge the support of the Academy of Finland Centre of Excellence program (project number 272041). V.V. acknowledges the financial support of the Nessling foundation (grant 201500326) and the Academy of Finland Finnish Center of Excellence program (grant 1118615). F.M. and T.R. acknowledges the financial support from the Academy of Finland ELTRAN (grant 293437).

Atmos. Chem. Phys. Discuss., doi:10.5194/acp-2015-990, 2016
Manuscript under review for journal Atmos. Chem. Phys.
Published: 5 February 2016

Atmospheric Chemistry and Physics Discussions

References

S. P. Arya, Modeling and parameterization of near-source diffusion in weak winds. J. Appl. Meteorol. 1995, 34, 1112-1122.

A. Awasthi, B.-S. Wu, C.-N. Liu, C.-W. Chen, S.-N. Uang and C.-J. Tsai. The effect of nanoparticle morphology on the measurement accuracy of mobility particle sizers. MAPAN-Journal of Metrology Society of India, 2013, 28(3), 205-215.

C.A. Brock, R.A. Washenfelder, M. Trainer, T.B. Ryerson, J.C. Wilson, J.M. Reeves, L.G. Huey, J. S. Holloway, D.D. Parrish, G. Hübler, F.C. Fehsenfeld. (2002) Particle growth in the plumes of coal-fired power plants. Journal of Geophysical Research, 2002, 107:D12, 4155.

G. Buonanno, P. Anastasi, F. DiIorio, A. Viola. Ultrafine particle apportionment and exposure assessment in respect of linear and point sources, Atmospheric Pollution Research, 2012, 1, 36-43.

T. Borsós, D. Řimnáčová, V. Ždímal, J. Smolík, Z. Wagner, T. Weidinger, J. Burkart, G. Steiner, G. Reischl, R. Hitzenberger, J. Schwarz, I. Salma. Comparison of particulate number concentration in three Central European capital cities. Science of the Total Environment, 2012, 433, 418-426.

R. J. Charlson, S. E. Schwartz, J. M. Hales, R. D. Cess, J. A. Coakley, Jr., J. E. Hansen and D. J. Hofmann. Climate Forcing by Anthropogenic Aerosols. Science New Series, 1992, Vol. 255, No. 5043, 423-430

EU, The EU Emissions Trading System (EU ETS), http://ec.europa.eu/clima/policies/ets/index_en.htm (accessed 15.12.2014)

A. K. Frey, K. Saarnio, H. Lamberg, F. Mylläri, P. Karjalainen, K. Teinilä, S. Carbone, J. Tissari, V. Niemelä, A. Häyrinen, J. Rautiainen, J. Kytömäki, P. Artaxo, A. Virkkula, L. Pirjola, T. Rönkkö, J. Keskinen, J. Jokiniemi, R. Hillamo. Optical and Chemical Characterization if Aerosols Emitted from Coal, Heavy and Light Fuel Oil, and Small-Scale Wood Combustion, Environmental Science & Technology, 2014, 48, 827-836.

J.J. Helble. A model for the air emissions of trace metallic elements from coal combustors equipped with electrostatic precipitators, Fuel Processing Technology, 2000, 63, 125-147.

R.-J. Huang, Y. Zhang, C. Bozzetti, K.-F. Ho, J.-J. Cao, Y. Han, K. R. Daellenbach, J. G. Slowik, S.M.Platt, F. Ganonaco, P. Zotter, R. Wolf, S. M. Pieber, E. A. Bruns, M. Grippa, G. Ciarelli, A. Piazzalunga, M. Schwikowsko, G. Abbaszade, J. Schnelle-Kreis, R. Zimmerman, Z. An, S. Szidat, U. Baltenspergerm I. El Haddad, A. S. H. Prévôt. High secondary aerosol contribution to particulate pollution during haze event in China, Nature, 2014, 514, 218-222.

Hofzumahaus, A., F. Rohrer, K. Lu, B. Bohn, T. Brauers, C.-C. Chang, H. Fuchs, F. Holland, K. Kita and Y. Kondo (2009). Amplified trace gas removal in the troposphere. Science 324(5935): 1702-1704

W. Junkermann, R. Hagemann, B. Vogel. Nucleation in the Karlsruhe plume during the COPS/TRACKS-Lagrange experiment. Quarterly Journal of the Royal Meteorological Society, 2011, 137, 267-274.

H. Junninen, A. Lauri, P. Keronen, P. Aalto, V. Hiltunen, P. Hari, M. Kulmala. Smart-SMEAR: on-line data exploration and visualization tool for SMEAR stations. Bor. Env. Res., 2009, 14, 447?457.

W. Klug. A method for determining diffusion conditions from synoptic observations, Staub-Reinhalt. Luft, 1969 29, pp. 14-20.

M. Kulmala, M. Dal Maso, J.M. Mäkelä, L. Pirjola, M. Väkevä, P. Aalto, P. Miikkulainen, K. Hämeri, C.D. O'Dowd. On the formation, growth and composition of nucleation mode particles. Tellus B, 2001, 53, 479?490.

Atmos. Chem. Phys. Discuss., doi:10.5194/acp-2015-990, 2016
Manuscript under review for journal Atmos. Chem. Phys.
Published: 5 February 2016

Atmospheric Chemistry and Physics Discussions

M. Kulmala, K.Lehtinen and A. Laaksonen. Cluster activation theory as an explanation of the linear dependence between formation rate of 3 nm particles and sulphuric acid concentration, Atmos. Chem. Phys., 2006, 6, pp. 787?793, doi:10.5194/acpd-6-787-2006.

S.W. Lee, T. Herage, R. Dureau, B. Young. Measurement of PM2.5 and ultra-fine particulate emissions from coal-fired utility boilers, Fuel, 2013, 108, 60-66.

K.E.J. Lehtinen, M. Dal Maso, M. Kulmala, V.-M. Kerminen. Estimating nucleation rates from apparent particle formation rates and vice versa: Revised formulation of the Kerminen-Kulmala equation. Journal of Aerosol Science, 2007, 38, 988?994.

Jos Lelieveld and Jost Heintzenberg. Sulfate Cooling Effect on Climate Through In-Cloud Oxidation of Anthropogenic SO2. Science New Series, 1992, Vol. 258, No. 5079, Genome Issue (Oct. 2, 1992), 117-120

M. Levin, A. Gudmundsson, J. H. Pagels, M. Fiers, K. Mølhave, J. Löndahl, K. A. Jensen, I. K. Koponen. Limitations in the Use of Unipolar charging for Electrical Mobility Sizing Instruments: A Study of the Fast Mobility Particle Sizer. Aerosol Science and Technology, 2013, 49, 556-565.

C.R. Lonsdal, R.G. Stevens, C.A. Brock, P.A. Makar, E.M. Knipping, J.R. Pierce. The effect of coal-fired power plant SO2 and NOx control technologies on aerosol nucleation in the source plumes. Atmos. Chem. Phys., 2012, 12, 11519-11531.

Lähde, T., Rönkkö, Virtanen, A., Schuck, T.J., Pirjola, L., Hämeri, K, Kulmala, M., Arnold, F., Rothe, D., Keskinen, J. (2009) Heavy duty diesel engine exhaust aerosol particle and ion measurements. Environ. Sci. Technol., 2009, 43 (1), 163-168.

H. Marris, K. Deboudt, P. Augustin, P. Flament, F. Blond, E. Fiani, M. Fourmentin, H. Delbarre. Fast changes in chemical composition and size distribution of fine particles during the near-field transport of industrial plumes. Science of the total Environment, 2012, 427-428, 126-138.

S. Mikkonen, S. Romakkaniemi, J.N.Smith, H. Korhonen, T. Petäjä, C. Plass-Duelmer, M. Boy, P.H. McMurry, K.E.J. Lehtinen, J. Joutsensaari, A. Hamed, R.L. Mauldin III, W. Birmili, G. Spindler, F. Arnold, M. Kulmala, A. Laaksonen. A statistical proxy for sulphuric acid concentration, Atmos. Chem. Phys., 2011, 11, 11319-11334.

F. Pasquill, The estimation of the dispersion of windborne material, The Meteorological Magazine, 1961, 90 (1063), pp 33-49.

Petäjä, T., Mauldin, III, R. L., Kosciuch, E., McGrath, J., Nieminen, T., Paasonen, P., Boy, M., Adamov, A., Kotiaho, T., and Kulmala, M.: Sulfuric acid and OH concentrations in a boreal forest site, Atmos. Chem. Phys., 9, 7435-7448, doi:10.5194/acp-9-7435-2009, 2009.

L. Pirjola, A. Pajunoja, J. Walden, J.-P. Jalkanen, T. Rönkkö, A. Kousa, T. Koskentalo 2014 Mobile measurements of shi emissions in two harbour areas in Finland, Atmos. Measu. Tech., vol 7, pp. 149-161.

L. Pirjola, M. Karl, T. Rönkkö, and F. Arnold. Model studies of volatile diesel exhaust particle formation: are organic vapours involved in nucleation and growth?, Atmospheric Chemistry and Physics, 2015, 13, 10435-10452.

T. Rönkkö, A. Arffman, P. Karjalainen, T. Lähde, J. Heikkilä, L. Pirjola, D.Rothe, J.Keskinen. Diesel exhaust nanoparticle volacity studies by a new thermodenuder with low solid nanoparticle losses, ETH Conference on Combustion Generated Nanoparticles, 2011.

Atmos. Chem. Phys. Discuss., doi:10.5194/acp-2015-990, 2016
Manuscript under review for journal Atmos. Chem. Phys.
Published: 5 February 2016

Atmospheric Chemistry and Physics Discussions

K. Saarnio, A. Frey, J.V. Niemi, H. Timonen, T. Rönkkö, P. Karjalainen, M. Vestenius, K. Teinilä, L. Pirjola, V. Niemelä, J. Keskinen, A. Häyrinen, R. Hillamo. 2014 Chemical composition and size of particles in emissions of coal-fired power plant with flue gas desulphurization, Journal of Aerosol Science, vol 73, 14-26.

J. H. Seinfeld, S.N. Pandis. Atmospheric chemistry and physics: from air pollution to climate change, second edition. John Wiley & Sons Inc., New York, 2006.

S.-L. Sihto, M. Kulmala, V.-M. Kerminen, M. Dal Maso, T. Petäjä, I. Riipinen, H. Korhonen, F. Arnold, R. Janson, M. Boy, A. Laaksonen, K. E. J. Lehtinen (2006) Atmospheric sulphuric acid and aerosol formation: implications from atmospheric measurements for nucleation and early growth mechanisms. Atmospheric Chemistry & Physics, 6, pp. 4079-4091.

R. K. Srivastava & W. Jozewicz (2001) Flue Gas Desulfurization: The State of the Art, Journal of the Air & Waste Management Association, 51:12, 1676-1688

R. G. Stevens and J. R. Pierce. A parameterization of sub-grid particle formation in sulfur-rich plumes for global- and regional-scale models, Atmos. Chem. Phys., 2013, 13, 12117-12133.

R.G. Stevens, J.R. Pierce, C.A. Brock, M.K. Reed, J.H. Crawford, J.S. Holloway, T.B. Ryerson, L.G. Huey, J.B. Nowak. Nucleation and growth of Sulfate aerosol in coal-fired power plant plumes: sensitivity to background aerosol and meteorology. Atmos. Chem. Phys., 2012, 12, 189-206

J. M. Stockie. The Mathematics of Atmospheric Dispersion Modeling, SIAM Review, 2011, Vol. 53, No. 2, pp. 349?372.

H. Yi, J. Hao, L. Duan, X. Tang, P. Ning, X. Li. Fine particle and trace element emissions from an anthracite coal-fired power equipped with bag-house in China, Fuel, 2008, 87, 2050-2057.